energies

MDPI

Article

A Robust-Based Home Energy Management Model for Optimal Participation of Prosumers in Competitive P2P Platforms

Alaa Al Zetawi [1], Marcos Tostado-Véliz [1,*], Hany M. Hasanien [2,3] and Francisco Jurado [1]

[1] Department of Electrical Engineering, University of Jaén, 23700 Linares, Spain; aa000177@red.ujaen.es (A.A.Z.); fjurado@ujaen.es (F.J.)
[2] Electrical Power and Machines Department, Faculty of Engineering, Ain Shams University, Cairo 11517, Egypt; hanyhasanien@ieee.org
[3] Faculty of Engineering and Technology, Future University in Egypt, Cairo 11835, Egypt
* Correspondence: mtostado@ujaen.es

Abstract: Nowadays, advanced metering and communication infrastructures make it possible to enable decentralized control and market schemes. In this context, prosumers can interact with their neighbors in an active manner, thus sharing resources. This practice, known as peer-to-peer (P2P), can be put into practice under cooperative or competitive premises. This paper focuses on the second case, where the peers partaking in the P2P platform compete among themselves to improve their monetary balances. In such contexts, the domestic assets, such as on-site generators and storage systems, should be optimally scheduled to maximize participation in the P2P platform and thus enable the possibility of obtaining monetary incomes or exploiting surplus renewable energy from adjacent prosumers. This paper addresses this issue by developing a home energy management model for optimal participation of prosumers in competitive P2P platforms. The new proposal is cast in a three-stage procedure, in which the first and last stages are focused on domestic asset scheduling, while the second step decides the optimal offering/bidding strategy for the concerned prosumer. Moreover, uncertainties are introduced using interval notation and equivalent scenarios, resulting in an amicable computational framework that can be efficiently solved by average machines and off-the-shelf solvers. The new methodology is tested on a benchmark four-prosumer community. Results prove that the proposed procedure effectively maximizes the participation of prosumers in the P2P platform, thus increasing their monetary benefits. The role of storage systems is also discussed, in particular their capability of increasing exportable energy. Finally, the influence of uncertainties on the final results is illustrated.

Keywords: home energy management; peer-to-peer; prosumer; smart home

Citation: Zetawi, A.A.; Tostado-Véliz, M.; Hasanien, H.M.; Jurado, F. A Robust-Based Home Energy Management Model for Optimal Participation of Prosumers in Competitive P2P Platforms. *Energies* **2024**, *17*, 5735. https://doi.org/10.3390/en17225735

Academic Editor: Guillermo Escrivá-Escrivá

Received: 30 October 2024
Revised: 13 November 2024
Accepted: 15 November 2024
Published: 16 November 2024

1. Introduction

1.1. Context and Motivation

With the advance of communication and metering infrastructures, the electricity sector is evolving towards more efficient and decentralized transaction paradigms. In such contexts, emerging concepts like energy communities, smart grids, and peer-to-peer (P2P) energy trading are gaining importance [1]. In particular, P2P energy exchanges among prosumers will play a crucial role in enhancing energy utilization in the residential sector. This paradigm enables energy exchanges among prosumers, thus allowing a more efficient utilization of surplus energy from rooftop photovoltaic (PV) units or battery energy storage (BES) systems [2].

From a conceptual point of view, P2P trades can be performed under a cooperative or competitive perspective [3]. In the former case, peers do not expect a monetary counterpart for energy exchanges with others [4]. In contrast, prosumers trade with other residential users on competitive platforms similarly to conventional energy markets [5].

This paper focuses on competitive P2P platforms, assuming that prosumers are capable of submitting bids and offers to an internal market infrastructure, where a coordinator seeks to maximize the collective welfare by updating individual spot prices. On such platforms, home energy management (HEM) systems are essential to effectively coordinate the different domestic assets. In consequence, such tools should be aware of possible opportunities brought from P2P trading and the behavior of other prosumers partaking in the platform. This paper focuses on this issue.

1.2. Literature Review

The literature regarding HEM is very rich, especially for the last five years (e.g., see [6]). The very first works focused on developing customized tools or mobile applications [7,8]. Later, HEM tools evolved toward incorporating users' preferences [9], lifestyle [10], demand response programs [11], uncertainties [12,13], or thermal comfort [14]. More recently, the literature regarding HEM systems has been particularly focused on modeling advanced thermostat models for heating–ventilation–air conditioner (HVAC) applications [15,16], incorporating vehicle-to-home capabilities [17–19], developing many-objective solution frameworks [20,21], or further modeling human behavior through predictive controllers [22]. Despite the huge amount of related works in the last years, the literature regarding HEM applications suitable for optimal participation in P2P platforms is still scarce.

Yang et al. presented a privacy-aware HEM system in [23]. This tool is suitable for P2P platforms where information exchanging may entail privacy concerns. To achieve a limited amount of public information, the developed tool is raised as a multi-objective optimization framework where, together with the minimization of the electricity bill, the problem seeks to minimize the number of features involved. In [24], a two-stage model for optimal P2P trading in a residential community was developed. Firstly, the problem focuses on P2P trading through a constrained non-linear model in which transaction prices are calculated using the modified supply–demand ratio method. At the second stage, a rule-based mechanism decides the appliances commitment, resulting in a sub-optimal but computationally friendly algorithm. A non-cooperative game-based P2P mechanism was proposed in [25] for residential communities. This mechanism is divided into sub-algorithms, competing the selling prices at first and the buyers' competition at second stage. However, HEM is not explicitly modeled, and only PV and BES domestic systems are included in the formulation.

In [3], an energy transaction mechanism among prosumers in cooperative communities was proposed. The proposed mixed-integer linear programming (MILP) methodology uses the alternating direction of multipliers to avoid sharing confidential information among users. Nevertheless, domestic assets are not comprehensively modeled, and only BES systems and fixed loads are considered. Feng et al. [26] proposed a coalitional game-based model for energy transactions in communities. Moreover, this paper considers uncertainty in renewable outputs using probability functions. Risk-seeker and risk-averse strategies are proposed in [27] for multi-microgrid systems. To this end, stochastic programming and information gap decision theory (IGDT) are hybridized to capture the uncertainty of renewable outputs, while cooperative energy transactions among microgrids are also included under a tractable MILP structure.

Jo et al. [5] focused on energy communities with large penetration of storage systems. In such systems, peers trade with their storage capacity within a local storage-based market mechanism coordinated by the community operator. A simple P2P-based model for residential communities was developed in [28], including uncertainties through stochastic programming. This work is presented for a benchmark three-building hydrogen-based community in which transactions among peers are performed cooperatively. A transactive framework for communities considering green and normal loads was proposed in [29]. In this model, the use of green loads is incentivized by means of demand response initiatives, while the depreciation cost of batteries is also considered. However, home components are not modeled in detail, and only PV systems and batteries are included in the formulation.

Energy transactions among peers in a local community are performed using a two-stage mechanism in [30]. In this reference, peers are modeled as strategic agents with the capability of adjusting their load profiles based on day-ahead electricity prices, which are decided through a bid-offer one-shot internal market mechanism.

Javadi et al. [31] developed a rule-based pool mechanism for surplus energy trading in communities. The model incorporates HEM models with price-based demand response programs incentivizing users to participate in P2P markets. In this work, preferences for controllable appliances (CAs) scheduling are modeled using probability distribution functions, resulting in a scenario-based approach. A two-stage energy management model for cooperative energy communities was developed in [4]. In this approach, electric vehicles (EVs), Cas, and BES systems are modeled as collective assets and scheduled with the aim of maximizing the collective welfare. Multiple uncertainties are modeled on a whole using interval notation and an original iterative algorithm, which allows to adopt pessimistic and optimistic points of view. A bock-based bilateral trading mechanism for nanogrids was proposed in [32]. This model aims to maximize the contract volume while preserving the privacy of users. To that end, a garbled circuit-based price comparison mechanism is proposed to compare prices and establishes a fair trading mechanism with limited information exchanging.

1.3. Contributions

Table 1 shows a summary of the related literature, including some remarks. Most of the related works are focused on cooperative P2P trading, in which peers do not expect any counterpart by sharing their resources. However, it is expected that competitive P2P platforms will gain importance to cooperative schemes for encouraging users to partake in P2P trades. In this regard, most of the existing works propose rule-based or other simple market mechanisms to decide P2P transactions or energy allocation among peers. In this regard, there is still a lack of research about fair price mechanisms for competitive P2P platforms, which is actually considered an open topic [33].

Table 1. A summary of the related literature.

Ref.	Model	Uncertainties	Remarks
[3]	MILP with alternating direction of multipliers	No	Branch losses are included as indirect costs while P2P transactions are cooperative
[4]	MILP, two-stage	Yes, using interval notation and iterative procedure	Domestic appliances and storage are modeled as collective assets and scheduled to maximize the collective welfare
[5]	MILP	No	Peers trade with storage capacity in a local market structure
[23]	Quadratic without explicitly modeling P2P trading	No	Focused on limiting the amount of information exchanged with the system
[24]	Non-linear/heuristic	No	Transaction prices are calculated using the modified supply–demand ratio method while appliances' scheduling is performed under rule-based decisions
[25]	Quadratic utility functions. Evolutionary game among buyers	No	Interactions among buyers and sellers are modeled using an M-leader and N-follower Stackelberg game approach
[26]	MILP with Coalitional game	Yes, using probability functions	Rayleigh distribution is used to capture uncertain in renewable outputs
[27]	MILP with cooperative P2P trading	Yes, using a stochastic-IGDT method	The original hybrid stochastic-IGDT formulation allows to adopt risk-seeker and risk-averse operational strategies
[28]	MILP with coordinator-ruled P2P transactions	Yes, using renewable scenarios	An electrolyzer and fuel-cell modeling are included in the formulation.
[29]	MILP with coordinator-ruled P2P transactions	No	Green and normal loads and prices are included together with storage depreciation cost.
[30]	MILP	No	Peers can trade energy in a P2P mechanism from which energy allocation is decided on the basis of bids from prosumers
[31]	MILP with rule-based P2P mechanism	No	A rule-based mechanism is proposed for P2P transactions while prosumers are encouraged to participate through demand response initiatives
[32]	MILP with garbled circuit	No	Privacy concerns are minimized using a garbled circuit-based price comparison mechanism is proposed based on a secure multi-party computation

Moreover, most of the literature regarding P2P transactions among prosumers is community-oriented rather than home-oriented. Clear examples are [3,4,29,31], where P2P transactions are decided centrally and coordinated collectively. In this sense, there is a need for developing a HEM-based mechanism for optimally participating in competitive P2P platforms. Note that in such a paradigm, prosumers can adopt different strategies and decisions from one peer that may affect others. In this sense, we believe it is necessary to develop an optimal offering strategy for prosumers participating in competitive P2P schemes, which requires adequate modelling of the different home assets since the effective coordination of such devices will determine the profit of users in P2P trading. Finally, most of the existing works neglect the uncertain effects introduced by renewable sources and random demand.

To fill the gaps above, this work develops a HEM tool suitable for participating in competitive P2P platforms. To this end, a three-stage methodology is developed, in which optimal appliance scheduling is decided firstly, with the aim of maximizing participation in P2P trading. Secondly, an optimal offering strategy is developed explicitly modeling P2P transactions among prosumers as well as individual prices and bids, for which a bi-level model is formulated and further converted into a single-level problem using the Karush–Kuhn–Tucker (KKT) conditions of the lower level. Finally, an adjusting mechanism is incorporated, taking into account the P2P result from the second stage. Furthermore, multiple uncertainties are modeled using interval notation and transformed into equivalent scenarios [34], thus resulting in an amicable framework that can be solved using off-the-shelf solvers. An illustrative four-prosumer case study is analyzed to validate the developed model.

In the rest of this paper, Section 2 presents the mathematical modeling of domestic assets. The bi-level model for P2P competitive trading is presented in Section 3 and further converting into a MILP single-level optimization problem. Section 4 develops a three-stage mechanism for optimal participation of prosumers in competitive P2P platforms. A case study with results is analyzed in Section 5, while the paper concludes with Section 6.

2. HEM Model

In this section, we briefly present the mathematical modeling of HEM assets. We consider a typical smart home encompassing a rooftop PV system, stationary batteries, EV bidirectional charger, Cas, and HVAC system [35]. Since this paper is home-oriented, the HEM formulation is presented for the i^* prosumer partaking in the P2P platform, for whom an optimal offering strategy is derived in Section 3. The formulation presented in this section has been widely employed and demonstrated in other references [11–13] and is adapted here to participation in P2P platforms.

2.1. Power Balance

Power balance in the home installation is ensured with (1). In this equation, $p_{i^*\leftarrow,t}$ and $p_{i^*\rightarrow,t}$ stand for the imported and exported power, respectively, from either P2P transactions or external agents (e.g., the distribution network). In particular, the left-hand side of (1) includes net generation by summing up the imported power, PV generation, and discharging power from storage assets (i.e., batteries and EVs). In contrast, the right-hand side of (1) comprises total demand, including exporting power, flexible and nonflexible loads, charging power from storage, and total HVAC consumption. In particular, the last term on the right-hand side calculates the total consumption of CAs, which are managed by commitment signals. On the other hand, (2) avoids simultaneous imports and exports ($\perp$ stands for complementarity). Actually, (2) is non-linear but easily linearizable, as described in Section 3.4.

$$\begin{aligned} p_{i^*\leftarrow,t} + p^{PV}_{i^*,t} + p^{BES,d}_{i^*,t} + p^{EV,d}_{i^*,t} \\ = p_{i^*\rightarrow,t} + p^{NC}_{i^*,t} + p^{BES,c}_{i^*,t} + p^{EV,c}_{i^*,t} + p^{HVAC,heat}_{i^*,t} + p^{HVAC,cool}_{i^*,t} \\ + \sum_{a\in\{\substack{\mathbb{A}^I_{i^*}\cup \\ \mathbb{A}^{NI}_{i^*}}\}} y^a_{i^*,t}\cdot p^a; \forall t\in\mathbb{T} \end{aligned} \tag{1}$$

$$0 \leq p_{i^*\leftarrow,t} \perp p_{i^*\rightarrow,t} \geq 0; \forall t \in \mathbb{T} \tag{2}$$

2.2. PV System

PV potential is determined by weather parameters, namely temperature and solar irradiance. Once these parameters have been estimated, the maximum instantaneous PV output (i.e., $\overline{p}^{PV}_{i^*,t}$) can be calculated using a suited model and panel characteristics [36,37], thus limiting the PV generation by (3).

$$p^{PV}_{i^*,t} \leq \overline{p}^{PV}_{i^*,t}; \forall t \in \mathbb{T} \tag{3}$$

2.3. Storage Systems

It is assumed that the EV is connected to the building through a bidirectional charger, which enables bidirectional power flow of on-board batteries. In this way, both stationary and vehicle batteries can be exploited as storage systems. In both cases, rated values bind exchanged power, as said (4), while (5) avoids unrealizable simultaneous charging/discharging (this equation can be linearized as (2)).

$$p^{x,c}_{i^*,t} \leq \overline{p}^{x},\ p^{x,d}_{i^*,t} \leq \overline{p}^{x}; \forall t \in \mathbb{T} \wedge x \in \{BES, EV\} \tag{4}$$

$$0 \leq p^{x,c}_{i^*,t} \perp p^{x,d}_{i^*,t} \geq 0; \forall t \in \mathbb{T} \wedge x \in \{BES, EV\} \tag{5}$$

Instantaneous state-of-charge (SOC) is given by (6), which results in linearizing the dynamic model of Li-ion batteries [38]. This equation models SOC at time t as a function of the total energy stored at time $t-1$, and the net energy exchanged with the system. On the other hand, SOC is upper and lower bounded with (7), considering total available capacity and depth-of-discharge settings.

$$\varepsilon^{x}_{i^*,t} = \varepsilon^{x}_{i^*,t-1} + \Delta t \cdot \left(\eta^{x}_{i^*} \cdot p^{x,c}_{i^*,t} - \frac{p^{x,d}_{i^*,t}}{\eta^{x}_{i^*}} \right); \forall t \in \mathbb{T} \backslash t > 1 \wedge x \in \{BES, EV\} \tag{6}$$

$$\underline{\varepsilon}^{x} \leq \varepsilon^{x}_{i^*,t} \leq \overline{\varepsilon}^{x}; \forall t \in \mathbb{T} \wedge x \in \{BES, EV\} \tag{7}$$

The main difference between BES and on-board batteries is their availability. While stationary batteries are always available, EV batteries can be only scheduled when the EV is plugged. In this regard, (8) and (9) avoid battery depletion by forcing initial and final SOC to be the same. In particular, it is worth noting that (9) forces on-board batteries to be fully charged before departing, assuming that the initial SOC of the EV is given by the parameter $\varepsilon^{EV}_{i^*,0}$, depending on the daily mileage [39]. Finally, (10) ensures that the vehicle cannot be charged/discharged when it is not plugged.

$$\varepsilon^{BES}_{i^*,\mathbb{T}[1]} = \varepsilon^{BES}_{i^*,|\mathbb{T}|} = \overline{\varepsilon}^{BES} \tag{8}$$

$$\varepsilon^{EV}_{i^*,\mathbf{\Theta}^{EV}_{i^*}[1]} = \varepsilon^{EV}_{i^*,0},\ \varepsilon^{EV}_{i^*,|\mathbf{\Theta}^{EV}_{i^*}|} = \overline{\varepsilon}^{EV} \tag{9}$$

$$p^{EV,x}_{i^*,t} = 0; \forall t \notin \mathbf{\Theta}^{EV}_{i^*} \wedge x \in \{c, d\} \tag{10}$$

Note that the BES model above does not consider possible thermal interactions inside battery systems [40] and only focuses on power interactions, which is a plausible assumption in energy management models devoted to power trading.

2.4. HVAC

To model the HVAC system, the indoor temperature is declared as an independent variable, which is affected by the outdoor temperature and the action of the HVAC devices as said (11) [11]. More specifically, (11) results of assuming a rectangular geometry for the building and linearized differential equations governing dynamic temperature, which is plausible under normal operating conditions. Furthermore, indoor temperature is kept

within comfortable limits using smart thermostats, as reflected in (12), while (13) establishes coherency in the model by forcing the initial and final temperatures to be the same. Heating and cooling modes cannot be activated simultaneously, as said (14) (this equation can be linearized as (2)), while (15) limits HVAC consumption, avoiding that thermostatically controlled devices import more power than their rated values.

$$\theta_{i^*,t}^{Air,in} = \theta_{i^*,t-1}^{Air,in} - \Delta t \cdot \left(\frac{\theta_{i^*,t-1}^{Air,out} - \theta_{i^*,t-1}^{Air,in}}{10^3 \cdot m^{Air,in} \cdot Q^{Air,in} \cdot R_{i^*}} + \frac{COP^{HVAC} \cdot (p_{i^*,t-1}^{HVAC,heat} + p_{i^*,t-1}^{HVAC,cool})}{0.000277 \cdot m^{Air,in} \cdot Q^{Air,in}} \right); \forall t \in \mathbb{T} \backslash t > 1 \quad (11)$$

$$\underline{\theta}_{i^*}^{Air,in} \leq \theta_{i^*,t}^{Air,in} \leq \overline{\theta}_{i^*}^{Air,in}; \forall t \in \mathbb{T} \quad (12)$$

$$\theta_{i^*,\mathbb{T}[1]}^{Air,in} = \theta_{i^*,|\mathbb{T}|}^{Air,in} = \theta^{HVAC,sp} \quad (13)$$

$$0 \leq p_{i^*,t}^{HVAC,heat} \perp p_{i^*,t}^{HVAC,cool} \geq 0; \forall t \in \mathbb{T} \quad (14)$$

$$p_{r|t}^{HVAC,x} \leq \overline{p}^{HVAC}; \forall t \in \mathbb{T} \wedge x \in \{heat, cool\} \quad (15)$$

2.5. CAs

As customary, CAs are divided into non-interruptible and interruptible [20]. In the former case, the operating cycle cannot be interrupted while interruptible appliances can be interrupted for convenience. In both cases, (16) ensures that duty cycles are completed within predefined time windows, i.e., CAs are forced to work a predefined number of hours in order to ensure that working cycles are completed while (17) and (18) ensure continuous operation of the non-interruptible appliances.

$$\sum_{t \in \Theta^a} y_{i^*,t}^a = \frac{DC^a}{\Delta t}; \forall a \in \left\{ \mathbb{A}_{i^*}^I \cup \mathbb{A}_{i^*}^{NI} \right\} \quad (16)$$

$$y_{i^*,t}^a - y_{i^*,t-1}^a = on_t^a - off_t^a; \forall t \in \mathbb{T} \backslash t < 1 \wedge a \in \mathbb{A}_{i^*}^{NI} \quad (17)$$

$$\sum_{t \in \mathbb{T}} on_t^a = 1; \forall a \in \mathbb{A}_{i^*}^{NI} \quad (18)$$

2.6. HEM Decision Variables

The HEM model is completed by declaring the vector of decision variables $\Xi_{i^*}^{HEM}$, which is defined in (19).

$$\Xi_{i^*}^{HEM} = \left\{ \begin{matrix} p_{i^* \leftarrow,t}, p_{i^* \rightarrow,t}, p_{i^*,t}^{x,d}, p_{i^*,t}^{x,c}, \\ p_{i^*,t}^{HVAC,heat}, p_{i^*,t}^{HVAC,cool}, \varepsilon_{i^*,t}^{x}, \\ \theta_{i^*,t}^{Air,in}, y_{i^*,t}^{a}, on_t^{aa}, off_t^{aa} \end{matrix} \right\}; \begin{matrix} \forall t \in \mathbb{T} \wedge a \in \left\{ \mathbb{A}_{i^*}^I \cup \mathbb{A}_{i^*}^{NI} \right\} \wedge \\ aa \in \mathbb{A}_{i^*}^{NI} \wedge x \in \{BES, EV\} \end{matrix} \quad (19)$$

3. Competitive P2P Modeling

The i^* prosumer described in the previous section partakes in a competitive P2P platform together with other peers gathered in $\mathbb{Q}$. These prosumers daily submit their buying/selling offers (given by the α's) which are collected by the P2P coordinator as represented in Figure 1. This agent determines the P2P trades among prosumers with the aim of maximizing the collective welfare and establishes energy prices between pairs of peers (given by the λ's).

Note that frequently prosumers are connected to existing networks through coupling converters. These devices enable smart control of power flows and establish advanced communication with other peers, thus making the proposed P2P platform feasible from a practical point of view. Nevertheless, it is out of the scope of this paper further discussing

necessary communication infrastructures and electronic interfaces, referring the interested reader to [41] for further information. Moreover, trading protocols should be enabled in order to provide fair and reliable transactions. In this regard, blockchain technologies could be enabled, as suggested in [42].

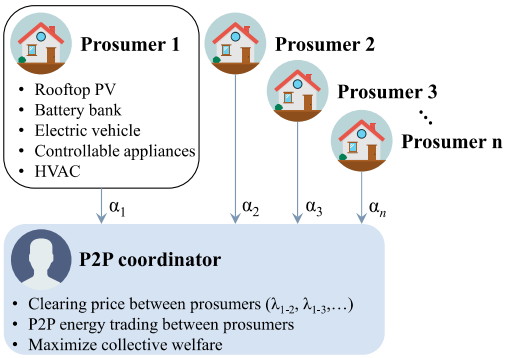

Figure 1. Scheme of the considered competitive P2P platform.

Subsequent sub-sections derive the optimal offering strategy for the i^* prosumer partaking in the competitive P2P platform sketched in Figure 1. Similar to other related problems, the mathematical formulation described below is cast as a bi-level problem and posteriorly transformed into a MILP single-level problem tractable by off-the-shelf solvers [43].

3.1. The Upper Level

The upper level describes the optimal bidding/offering for the i^* prosumer in the platform. Thus, this level decides on the price bid submitted to the P2P coordinator to reveal local prices, with the objective of maximizing the prosumer profit. In this paper, the profit for the i^* prosumer results of trading energy with the other peers under local prices, as said (20).

$$\underset{\substack{\alpha^{P2P}_{i^*,t} \geq 0, p^{P2P}_{i^*\rightarrow j,t}, p^{P2P}_{i^*\leftarrow j,t};\\ \forall j \in \mathbb{Q} \backslash j \neq i^* \wedge t \in \mathbb{T}}}{max} \Delta t \cdot \sum_{t\in\mathbb{T}} \sum_{\substack{j\in\mathbb{Q}\\ j\neq i^*}} \left\{ \lambda^{P2P}_{i^*-j,t} \cdot \begin{pmatrix} p^{P2P}_{i^*\rightarrow j,t} \\ -p^{P2P}_{i^*\leftarrow j,t} \end{pmatrix} \right\} \tag{20}$$

3.2. The Lower Level

In the lower level, the P2P manager coordinates energy trading among prosumers while clearing local prices between peers. The objective of this level is maximizing the social welfare (21), subject to (22)–(24).

$$\underset{\substack{p^{P2P}_{i\rightarrow j,t}, p^{P2P}_{i\leftarrow j,t};\\ \forall i,j \in \mathbb{Q} \wedge t \in \mathbb{T}}}{max} \Delta t \cdot \sum_{t\in\mathbb{T}} \sum_{\substack{j\in\mathbb{Q}\\ j\neq i}} \left\{ \sum_{j\in\mathbb{Q}} \left\{ \alpha^{P2P}_{i,t} \cdot \left(p^{P2P}_{i\leftarrow j,t} - p^{P2P}_{i\rightarrow j,t} \right) \right\} \right\} \tag{21}$$

Subject to the following:

$$\sum_{\substack{j\in\mathbb{Q}\\ j\neq i}} p^{P2P}_{i\rightarrow j,t} \leq \overline{p}_{i\rightarrow,t}, \sum_{\substack{j\in\mathbb{Q}\\ j\neq i}} p^{P2P}_{i\leftarrow j,t} \leq \overline{p}_{i\leftarrow,t} : \overline{\mu}_{i\rightarrow,t}, \overline{\mu}_{i\leftarrow,t}; \forall i \in \mathbb{Q} \wedge t \in \mathbb{T} \tag{22}$$

$$0 \leq p^{P2P}_{i\rightarrow j,t}, 0 \leq p^{P2P}_{i\leftarrow j,t} : \underline{\mu}_{i\rightarrow j,t}, \underline{\mu}_{i\leftarrow j,t}; \forall i,j \in \mathbb{Q} \backslash j \neq i \wedge t \in \mathbb{T} \tag{23}$$

$$p^{P2P}_{i\rightarrow j,t} - p^{P2P}_{j\leftarrow i,t} = 0 : \lambda^{P2P}_{i-j,t}; \forall i,j \in \mathbb{Q} \backslash j \neq i \wedge t \in \mathbb{T} \tag{24}$$

In the model above, (22) binds individual power traded, imposing power limits, which are submitted to each peer individually. On the other hand, (23) forces power traded to

be greater than zero in order to avoid unrealizable solutions. Finally, (24) establishes the power balance between pairs of peers [3]. In the model (22)–(24), dual variables are written in the right-side of each equation. As seen, the energy price between pairs of prosumers is derived from (24), thus reflecting local marginal costs as customary in marginal-based market mechanisms.

3.3. Mathematical Programming with Complementarity Constraints (MPCC)

The optimization model (20)–(24) constitutes a bi-level framework whose solution is NP-hard [44]. Different approaches have been proposed to find solutions to bi-level problems efficiently. When the lower level problem is linear (and therefore convex), bi-level optimization models can be reduced to solvable single-level ones easily. This solution strategy has multiple advantages. Firstly, it allows solving the model using off-the-shelf solvers. Secondly, the solution achieved is ensured to be an equilibrium point in the Nash sense. As commented, since the lower level is continuous and linear, it can be replaced by its equivalent KKT conditions, which can be added to the upper level to form a single-level MPCC framework [45]. The MPCC model envisaged from (21)–(24) is given by (25)–(28), where (25) and (26) are the stationary conditions derived from the Lagrangian function of (21) (see Appendix A), the complementarity conditions are given in (27) and (28) and (29) is the dual feasibility constraint (the interested reader is referred to [46] for a further explanation above how to derive KKT conditions of linear models).

$$\alpha_{i,t}^{P2P} + \lambda_{i-j,t}^{P2P} - \underline{\mu}_{i\rightarrow j,t} + \overline{\mu}_{i\rightarrow,t} = 0;\ \forall i,j \in \mathbb{Q} \backslash j \neq i \wedge t \in \mathbb{T} \tag{25}$$

$$-\alpha_{i,t}^{P2P} - \lambda_{i-j,t}^{P2P} - \underline{\mu}_{i\leftarrow j,t} + \overline{\mu}_{i\leftarrow,t} = 0;\ \forall i,j \in \mathbb{Q} \backslash j \neq i \wedge t \in \mathbb{T} \tag{26}$$

$$\begin{aligned} 0 \leq \overline{\mu}_{i\rightarrow,t} \perp \left(\overline{p}_{i\rightarrow,t} - \sum_{\substack{j\in\mathbb{Q} \\ j\neq i}} p_{i\rightarrow j,t}^{P2P} \right) \geq 0 \\ 0 \leq \overline{\mu}_{i\leftarrow,t} \perp \left(\overline{p}_{i\leftarrow,t} - \sum_{\substack{j\in\mathbb{Q} \\ j\neq i}} p_{i\leftarrow j,t}^{P2P} \right) \geq 0 \end{aligned} \quad ;\ \forall i \in \mathbb{Q} \wedge t \in \mathbb{T} \tag{27}$$

$$\begin{aligned} 0 \leq \underline{\mu}_{i\rightarrow j,t} \perp p_{i\rightarrow j,t}^{P2P} \geq 0 \\ 0 \leq \underline{\mu}_{i\leftarrow j,t} \perp p_{i\leftarrow j,t}^{P2P} \geq 0 \end{aligned} ;\ \forall i,j \in \mathbb{Q} \backslash j \neq i \wedge t \in \mathbb{T} \tag{28}$$

$$\underline{\mu}_{i\rightarrow j,t}, \overline{\mu}_{i\rightarrow,t}, \underline{\mu}_{i\leftarrow j,t}, \overline{\mu}_{i\leftarrow,t} \geq 0 \tag{29}$$

Thus, the MPCC problem resulting from integrating (25)–(28) into the upper level is given by the following:

Objective function: (20)
Subject to (25)–(29).

3.4. MILP

The MPCC problem defined in the previous sub-section presents non-linearities in the complementarity constraints (27) and (28), as well as in the objective function (20). To linearize complementarity constraints, the big-M method (30) can be used.

$$0 \leq \delta_1 \perp \delta_2 \geq 0 \cong \begin{cases} \delta_1 \geq 0, \delta_2 \geq 0 \\ \delta_1 \leq \psi \cdot M \\ \delta_2 \leq (1-\psi) \cdot M \\ \psi \in \{0,1\} \end{cases} \tag{30}$$

where the δ's are the two terms involved in a complementarity constraint, ψ is a binary variable (different binary variables must be declared for each complementarity constraint),

and M is a large number. Note that (30) is also valid for linearizing the complementarity constraints in the HEM model (2), (5), and (14). It is worth mentioning that fixing M is not a trivial problem and may entail ill-conditioning issues [47]. However, preliminary experiments showed that this parameter can be defined coarsely as ~10^5 for the problem considered in this paper.

On the other hand, the strong duality theorem is used to linearize (20). This principle establishes that the value of the objective function and its dual are exactly the same in the optimal point [48]. This way, (20) can be replaced by the linear term in the right side of (31) (see Appendix B).

$$\Delta t \cdot \lambda^{P2P}_{i^*-j,t} \cdot \left(p^{P2P}_{i^*\rightarrow j,t} - p^{P2P}_{i^*\leftarrow j,t} \right) = \Delta t \cdot \sum_{t\in\mathbb{T}} \left\{ \begin{array}{l} \sum\limits_{\substack{i\in\mathbb{Q} \\ i\neq i^*}} \sum\limits_{\substack{j\in\mathbb{Q} \\ j\neq i^*}} \alpha^{P2P}_{i,t} \cdot \left(p^{P2P}_{i\leftarrow j,t} - p^{P2P}_{i\rightarrow j,t} \right) + \\ \sum\limits_{\substack{i\in\mathbb{Q} \\ i\neq i^*}} \left\{ \overline{\mu}_{i\rightarrow,t} \cdot \overline{p}_{i\rightarrow,t} + \overline{\mu}_{i\leftarrow,t} \cdot \overline{p}_{i\leftarrow,t} \right\} \end{array} \right\} \quad (31)$$

4. The Developed Solution Procedure

Sections 2 and 3 establish independent problems. However, this paper aims to present a holistic framework in which the HEM problem is integrated into the optimal offering strategy described in Section 3. To this end, a three-stage procedure is developed, which is summarized in the flowchart of Figure 2. Firstly, the HEM problem given in Section 2 is performed daily, from which the maximum importable/exportable power for the i^* prosumer is obtained. This information is transferred to the competitive P2P problem described in Section 3, where the i^* prosumer decides his optimal offering strategy for the following 24 h. Finally, the HEM scheduling plan is readjusted considering the P2P transactions determined at Stage 2. At this stage, HEM-related uncertainties are accommodated using interval notation and equivalent scenarios [34].

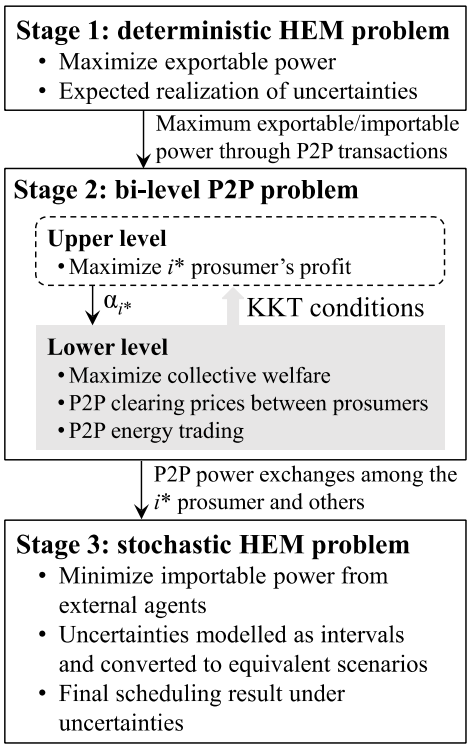

Figure 2. Flowchart of the developed solution procedure.

4.1. Stage 1

The proposed P2P platform aims at maximizing social welfare, to which each prosumer needs to submit her offer/bid but also her maximum exportable/importable power for any instance of time. Note that this information is valuable for the market operator in order to determine whether a particular prosumer can partake as a load (importing energy from the market) or as a generator (delivering power to the market). To determine this information, Stage 1 solves the HEM problem with the objective of maximizing the importable/exportable power, subjected to the particular constraints in the HEM model considering controllable appliances, etc. Keeping this in mind, Stage 1 is written as follows:

$$\overline{p}_{i^*\rightarrow,t}, \overline{p}_{i^*\leftarrow,t} \in \underset{\Xi_{i^*}^{HEM}}{max} \Delta t \cdot \sum_{t\in\mathbb{T}} p_{i^*\rightarrow,t} \tag{32}$$

Subject to (1)–(18).

As seen above, (32) maximizes the participation of the prosumer i^* in the market by maximizing the power exchanged. As a result, power bounds $\overline{p}_{i^*\rightarrow,t}$ and $\overline{p}_{i^*\leftarrow,t}$ are submitted to Stage 2, where the market clearing problem is solved. On the other hand, constraints (1)–(18) ensure physically realizable solutions.

4.2. Stage 2

The second stage corresponds with the market clearing problem, by which the market coordinator clears local prices with the objective of maximizing the collective welfare. This stage requires information about maximum importable/exportable power of each prosumer. For the prosumer i^*, this information is obtained after solving the Stage 1, while bounds for the rival prosumers need to be estimated. In this stage, the prosumer i^* determines her optimal bidding/offering strategy to maximize her profit in the P2P market. Mathematically, this problem casts as a bi-level framework that can be reduced into a single-level one, as explained in Section 3, thus written as follows:

$$\begin{array}{c} \underset{\substack{\alpha_{i^*,t}^{P2P}, p_{i\rightarrow j,t}^{P2P}, p_{i\leftarrow j,t}^{P2P},\\ \lambda_{i-j,t}^{P2P}, \overline{\mu}_{i\rightarrow,t}, \overline{\mu}_{i\leftarrow,t},\\ \underline{\mu}_{i\rightarrow j,t}, \underline{\mu}_{i\leftarrow j,t}, \psi's;\\ \forall i,j \in \mathbb{Q} \wedge t \in \mathbb{T}}}{max} \\ \Delta t \cdot \sum_{t\in\mathbb{T}} \left\{ \begin{array}{l} \sum\limits_{\substack{i\in\mathbb{Q}\\ i\neq i^*}} \sum\limits_{\substack{j\in\mathbb{Q}\\ j\neq i^*}} \alpha_{i,t}^{P2P} \cdot \left(p_{i\leftarrow j,t}^{P2P} - p_{i\rightarrow j,t}^{P2P} \right) + \\ \sum\limits_{\substack{i\in\mathbb{Q}\\ i\neq i^*}} \left\{ \overline{\mu}_{i\rightarrow,t} \cdot \overline{p}_{i\rightarrow,t} + \overline{\mu}_{i\leftarrow,t} \cdot \overline{p}_{i\leftarrow,t} \right\} \end{array} \right\} \end{array} \tag{33}$$

Subject to (24)–(26), (29), and (30).

The social welfare (21) is calculated as the area between the bid-offer curve, in line with conventional wholesale energy markets. However, (33) is an equivalent linear counterpart deduced from the strong-duality theorem, as detailed in Appendix B.

4.3. Stage 3

HEM problems are subjected to multiple uncertainties brought by non-controllable demand, uncertain PV generation, or the initial SOC of the EV [13]. Different approaches have been proposed in the literature to address uncertainties in optimization problems, which may be broadly categorized as scenario-based or robust approaches. Scenario-based (also referred to as stochastic) fashions uncertainties by means of scenarios, catching possible realizations of uncertain parameters. These approaches are simple but typically incur computational issues [49]. In this regard, robust approaches have been preferred in this paper. In particular, we consider interval notation of uncertainties, by which a given uncertainty φ can be represented by its expected value and confidence intervals, as follows:

$$\varphi \in [E(\varphi) \cdot (1-\xi), E(\varphi) \cdot (1+\xi)] \tag{34}$$

where $\xi \in \mathbb{R}^+$ is the so-called uncertain level [50], which represents the deviation of the parameter φ with respect to its expected value. Indeed, interval numbers in the form of (34) model deviation of uncertain parameters from their expected values. In this regard, the uncertain level makes the optimization model adaptive. As seen, tuning $\xi = 0$ equivalates to assume deterministic conditions, as φ is forced to be equal to its expected value. On the other hand, incrementing the value of the uncertain parameters leads to considering wide ranges, and therefore the parameter may implicitly deviate longer from its forecasted profile, eventually leading to robust results. Thus, tuning ξ is actually a case-dependent task and depends, mainly, on the risk-aware strategy adopted by users. If the users are highly risk-aware, high values of ξ should be adopted. Therefore, the value of the uncertainty level can be considered as a quantification of the uncertainties in the model. Indeed, the results become more risk-aware as higher values of ξ are taken.

Normally, interval numbers are not easily accommodated in MILP frameworks [51]. To solve this issue, we follow the procedure described in [52], by which an interval number defined by its expected value and upper/lower bounds can be replaced by three equi-probable scenarios (i.e., $\Omega_\varphi = \{\mathrm{E}(\varphi)\cdot(1-\xi), \mathrm{E}(\varphi), \mathrm{E}(\varphi)\cdot(1+\xi)\}$). In this sense, continuous variables in $\Xi_{i^*}^{HEM}$ extend for one more dimension ω for each scenario. Now, it is necessary to determine the worst/best realization of each uncertainty in order to associate corresponding scenarios. This is an easy task in HEM problems since while the best scenario for the PV generation and initial EV SOC is always linked with their upper bounds, the best case for the non-controllable demand is given for its lower bound. Nevertheless, the worst-case realization for the outdoor temperature may be difficult to know a priori, since both low and high temperatures may result in a more continuous operation of the HVAC unit. To determine the worst scenario for the outdoor temperature, we propose to calculate the total heating/cooling energy dedicated in HVAC processes after running the first stage. If the heating energy is higher than the cooling energy, then the worst case for the outdoor temperature coincides with its lower bound, taking the upper limit otherwise.

In this stage, P2P transactions are taken into account when readjusting the domestic assets. Thus, the power balance (1) is replaced by (34), which includes the P2P imports and exports.

$$\begin{aligned} p_{i^*\leftarrow j,t}^{P2P} + p_{i^*,\omega,t}^{Ext} + p_{i^*,\omega,t}^{PV} + p_{i^*,\omega,t}^{BES,d} + p_{i^*,\omega,t}^{EV,d} \\ = p_{i^*\rightarrow j,t}^{P2P} + p_{i^*,\omega,t}^{NC} + p_{i^*,\omega,t}^{BES,c} + p_{i^*,\omega,t}^{EV,c} + p_{i^*,\omega,t}^{HVAC,h} + p_{i^*,\omega,t}^{HVAC,c} \\ + \sum_{a\in\{\substack{\mathbb{A}_{i^*}^{I}\cup \\ \mathbb{A}_{i^*}^{NI}\}}} y_{i^*,t}^{a}\cdot p^{a}; \forall\omega\in\Omega\wedge t\in\mathbb{T} \end{aligned} \tag{35}$$

In (35), $p_{i^*,\omega,t}^{Ext}$ reflects the power that cannot be accommodated by either on-site generators or P2P trades and therefore must be acquired from external entities (e.g., the distribution network). Thus, the objective of this stage is minimizing the energy purchased from external systems, assuming that it is typically purchased at high cost. Thereby, Stage 3 is defined as follows:

$$\min_{\Xi_{i^*,\mathbf{\Omega}}^{HEM}} \Delta t\cdot\sum_{\omega\in\Omega}\left\{\frac{1}{|\Omega|}\cdot\sum_{t\in\mathbb{T}} p_{i^*,\omega,t}^{Ext}\right\} \tag{36}$$

Subject to (2)–(18) and (35)

where $\Xi_{i^*,\mathbf{\Omega}}^{HEM}$ is the vector of decision variables for the third stage resulting of extending $\Xi_{i^*}^{HEM}$ over the scenario set $\mathbf{\Omega}$ given by the following:

$$\Xi_{i^*,\mathbf{\Omega}}^{HEM} = \left\{\begin{matrix} p_{i^*,\omega,t}^{Ext}, p_{i^*,\omega,t}^{x,d}, p_{i^*,\omega,t}^{x,c}, \\ p_{i^*,\omega,t}^{HVAC,heat}, p_{i^*,\omega,t}^{HVAC,cool}, \varepsilon_{i^*,\omega,t}^{x}, \\ \theta_{i^*,\omega,t}^{Air,in}, y_{i^*,t}^{a}, on_{t}^{aa}, off_{t}^{aa} \end{matrix}\right\}; \begin{matrix} \forall\omega\in\Omega\wedge t\in\mathbb{T}\wedge a\in\left\{\mathbb{A}_{i^*}^{I}\cup\mathbb{A}_{i^*}^{NI}\right\}\wedge \\ aa\in\mathbb{A}_{i^*}^{NI}\wedge x\in\{BES, EV\} \end{matrix} \tag{37}$$

5. Case Study

This section presents a case study with results. The MILP model described in previous sections has been coded under Matlab R2021a and solved using Gurobi [53]. All simulations were run over a 24 h time horizon with 1 h time resolution.

5.1. Input Data and Cases Studied

An illustrative four-prosumer platform has been taken as a benchmark case study. We consider that $i^* = 1$, and therefore prosumer #1 enables his optimal offering/bidding strategy using the developed three-stage procedure. To illustrate and further validate the developed methodology, two cases are analyzed:

- Case 1: It is considered a low-renewable scenario in which the studied prosumer does not install onsite generators, and therefore PV potential is equal to zero.
- Case 2: It is considered a high renewable scenario in which the studied prosumer installs a 2.5 kWp PV array which, considering the weather data reported in [20], yields the PV potential plotted in Figure 3.

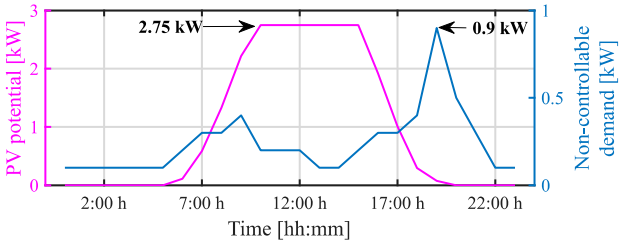

Figure 3. PV potential and non-controllable demand for the studied prosumer.

The non-controllable demand for the analyzed prosumer is plotted in Figure 3 and is based on the data in [20]. Table 2 contains the data regarding BES, EV, and HVAC, while parameters of CAs are reported in Table 3. These parameters correspond to typical data of smart prosumers installing PV, BES, HVAC and EV, and are in line with other references like [4,13]. On the other hand, the estimated importable/exportable powers and offers/bids from other peers are plotted in Figure 4.

Table 2. Data of domestic assets.

Parameter	Value	Parameter	Value
$\overline{\varepsilon}^{BES}/\underline{\varepsilon}^{BES}/\overline{\varepsilon}^{EV}/\underline{\varepsilon}^{EV}$ [kWh]	5/1/16/3.2	$Q^{Air,in}$ [kJ/(kg·°C)]	1.01
$\overline{p}^{BES}/\overline{p}^{EV}/\overline{p}^{HVAC}$ [kW]	2/3.7/2	R [J/°C]	$3.2{\cdot}10^{-6}$
$\overline{\theta}^{Air,in}/\underline{\theta}^{Air,in}/\theta^{HVAC,sp}$ [°C]	22.5/23.5/23	COP^{HVAC} [-]	1.2
η^{BES}/η^{EV} [%]	95/95	$\mathbf{\Theta}_1^{EV}$	0:00–9:00 h
$m^{Air,in}$ [kg]	1500	$\varepsilon_{1,0}^{EV}$ [kWh]	9.6

Table 3. Data of CAs.

Power [kW]	Duty Cycle [h]	Time Window	Type
2	4	4:00–20:00 h	Non-interruptible
1.2	3	6:00–22:00 h	Interruptible
0.5	2	16:00–23:00 h	Non-interruptible

5.2. Results

Table 4 reports the total importable/exportable energy in the two case studies. This result is obtained after running Stage 1 of the developed methodology, when the prosumer aims at maximizing his participation in P2P transactions by augmenting his exportable energy. As observed, the presence of PV panels allows us to export much more energy, but

also the importable energy is reduced. To obtain a better view of these results, Figure 5 shows the scheduling result for the domestic assets. As seen, the maximum importable power occurs in the early morning in the two studied cases, when the EV needs to be charged. However, there is another 6.9 kW peak period in the evening in case 1. This is due to, in the presence of PV generation, the HEM scheduler translates the operation of CAs out of the central hours of the day, when the PV potential is high and can be exploited for incrementing the exportable power. In both cases, the maximum exportable power occurs at noon, propitiated by discharging the on-board batteries. Note that bi-directional charges allow 3.7 kW of power flow to the community, which, combined with BES discharging, allows us to export more than 5 kW at 3:00 h.

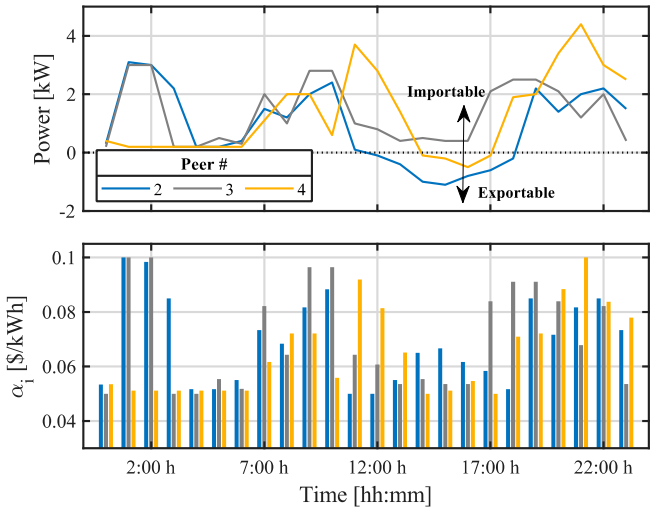

Figure 4. Estimated importable/exportable powers (**top**) and offers/bids (**bottom**) from other peers.

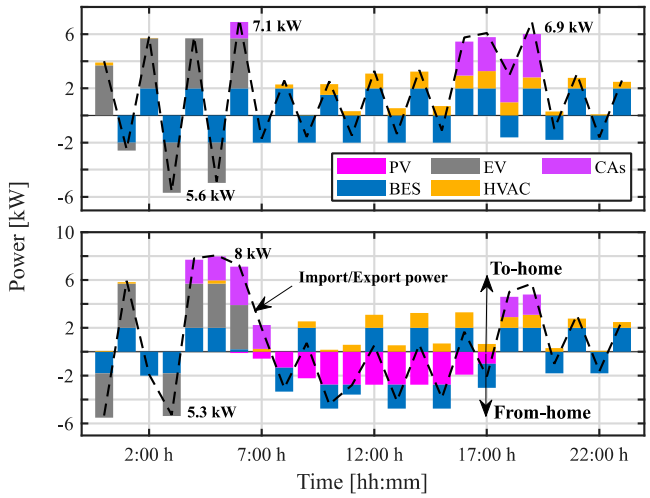

Figure 5. Scheduling result for the studied prosumer in case 1 (**top**) and case 2 (**bottom**).

Table 4. Total importable/exportable energy for the studied prosumer.

Result	Case 1	Case 2
Total importable	61.75 kWh	50.80 kWh (−21.5%)
Total exportable	22.86 kWh	35.40 kWh (+35.4%)

After running Stage 1, P2P trades are decided at Stage 2. Figure 6 shows the chord diagrams for the P2P transactions that occurred in the studied cases. As seen, peers 1 and 2 exchange a huge amount of energy (3.3 kWh and 2.8 kWh in cases 1 and 2, respectively), while

much less energy is traded between peers 2 and 3 (0.4 kWh and 0.8 kWh in cases 1 and 2, respectively) and peers 3 and 4 (0.8 kWh in cases 1 and 2). To understand this result, Figure 7 plots the instantaneous transactions among peers occurred in the two studied cases. As observed, results reported in Figure 6 are mainly due to the transactions that occurred at noon between peers 1 and 2, when peer 1 exported 2.2 kW to peer 1. At 3:00 h, the energy demanded by peer 2 was totally covered by importing energy from peer 1, who is able to export much energy by discharging on-board batteries, as explained in Figure 5. The rest of the trades mainly take place in the afternoon due to the high PV generation. In case 1, peers 1 and 3 cannot export energy and therefore they import from peers 2 and 4, who are capable of exporting energy as seen in Figure 4. In case 2, peer 1 does not require imported energy from others since his demand can be satisfied by means of his own PV generation.

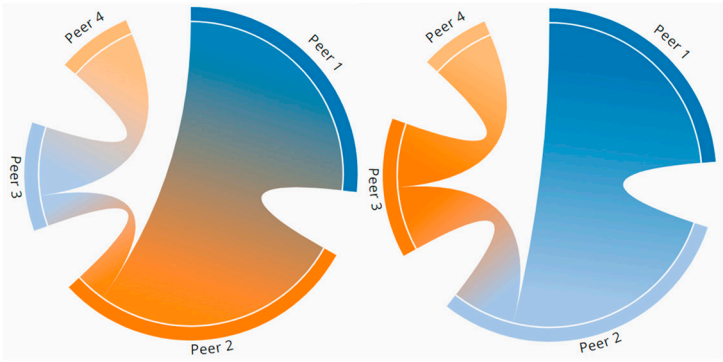

Figure 6. Scheduling result for the studied prosumer in case 1 (**left**) and case 2 (**right**).

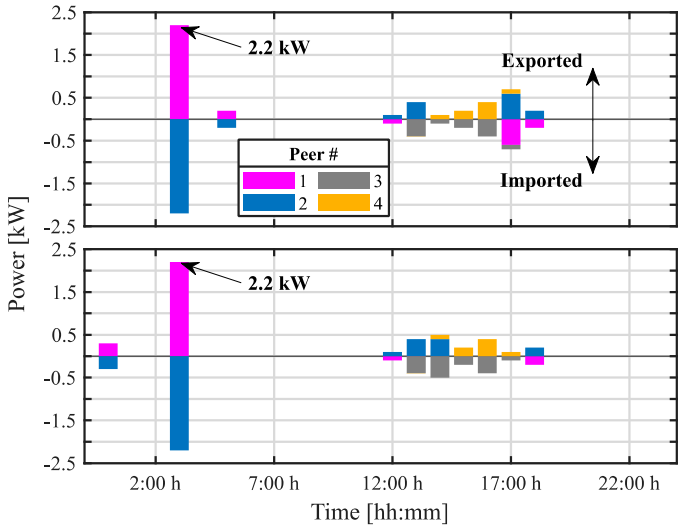

Figure 7. P2P transactions in case 1 (**top**) and case 2 (**bottom**).

The results above strengthen the importance of properly scheduling the domestic assets to optimally partake in competitive P2P platforms. Indeed, in this case, peer 1 has an advantage over the others since, while the rest of peers cannot export energy at noon, the studied peer is able to export energy by discharging batteries and thus enable P2P trades with other peers. It is worth noting that total energy exchanged through P2P trades does not notably vary in each case. In fact, the total energy exchanged between peers 1 and 2 decreases in case 2. This is due to, in the presence of PV panels, peer 1 maximizes his total exportable energy and reduces the importable necessities. Thus, the studied peer does not require to import energy from the P2P platform, being able to satisfy his own demand through onsite PV generation. This result evidences that the developed methodology aims

at maximizing the participation of peers in the P2P platform by only exporting energy, since thus hidden monetary opportunities can be enabled and the monetary balance is improved.

Figure 8 shows the clearing prices between pairs of prosumers (for the sake of simplicity, only results for case 1 are plotted, while similar results can be extracted for case 2). At 3:00 h, when peer 2 imports energy from peer 1, the P2P coordinator equals λ_{1-2} to the bidding price of peer 2, thus maximizing the welfare of both peers. In the afternoon, peer 3 imports power from peers 2 and 4. During these hours, λ_{2-3} and λ_{3-4} fall since there is a clear excess of energy in the community, allowing peer 3 to purchase energy at low prices. During these hours, the prices of peers 2, 3, and 4 are also low, thus maximizing the collective welfare. As seen, prosumers impact local prices mainly in two ways. On the one hand, by means of their bids submitted, and, on the other hand, by providing low-cost renewable generation. Actually, renewable generation allows reducing prices in λ_{2-3} at midday. The results in Figure 8 show a clear marginal-oriented market environment, which faithfully reflects the instantaneous total generation cost. This pricing mechanism is considered suitable for energy markets and is widely used in practice.

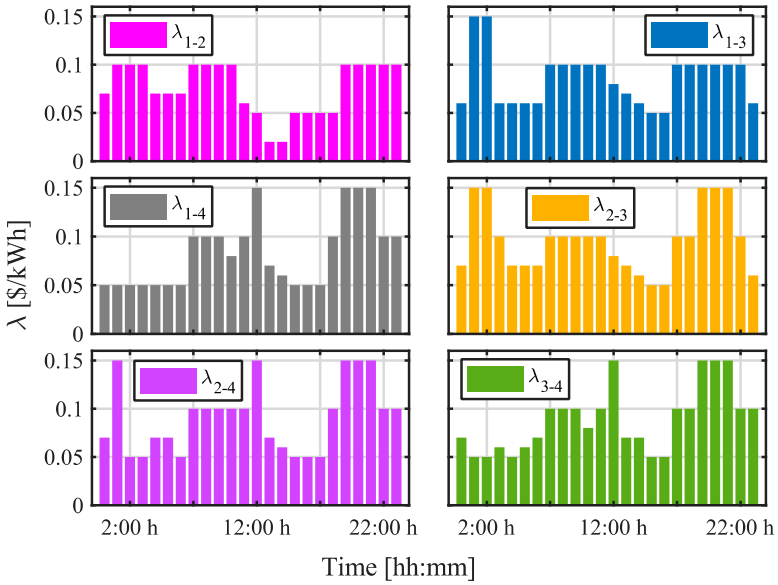

Figure 8. Clearing prices for P2P transactions in case 1.

Figure 9 shows the pricing strategy of the studied peer (peer 1). At 3:00 h, when he exports power to peer 2, his offering price (0.1 $/kWh) is almost equal to the bid launched by peer 2 (0.09 $/kWh). In this situation, the coordinator clears at 0.1 $/kWh. At 17:00 h, when peer 1 imports energy from peer 2, the studied prosumer bids 0.1 $/kWh, much higher than the offer of peer 2 (0.06 $/kWh), being the clearing price fixed at 0.1 $/kWh. This way, peer 1 ensures that he acquires energy from the P2P transactions.

After matching energy from P2P trades, the remainder of the importable necessities must be covered by importing power from external agents. This is scheduled at Stage 3, when uncertainties are also included. In this regard, Figure 10 plots the total energy that must be acquired from external systems (i.e., external energy) for different values of the uncertain level (ξ). As seen, the total external energy increases with the value of the uncertain level in both the worst and expected scenarios. In the former case, this is undoubtedly due to the unfavorable trend of uncertainties, which are assumed to deviate from the expected profile in a pessimistic way. In the expected scenario, uncertainties take their forecasted values, and therefore the results should not be affected by the value of ξ. However, it is worth noting that the commitment statuses for domestic assets do not vary for each scenario (the y's have no dimension ω), and therefore their scheduling affects the three contemplated scenarios, disregarding the assumed value of uncertainties. On the other hand, the total external energy increases with the value of ξ for the best scenario in

case 1, while it decreases in case 2. This is due to the presence of PV generation in case 2. Indeed, optimistic deviation assumed for PV generation compensates the scheduling result for commitment statuses and the total external energy is thus reduced, which does not occur in the case 1, where the y's are decided to minimize the objective function over the three contemplated scenarios, as explained before. It is also worth noting that the total external energy increases more notably in the worst scenario for case 2, especially for $\xi > 0.4$. This is due to, together with the pessimistic value of uncertainties, low PV potential is also assumed, which leads to a very pessimistic scenario. Nevertheless, results obtained for case 2 were better than those obtained in case 1, as expected, since the presence of PV units reduces the necessity of purchasing energy from external agents. It is worth noting that tuning $\xi = 0$ equivalates to the deterministic model in which uncertainties are forced to be equal to expected values. Under these assumptions, total external energy does not vary in each case, which is coherent and further validates the developed model.

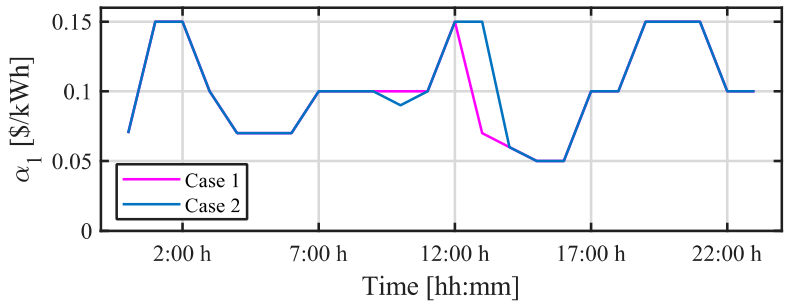

Figure 9. Offering prices for peer 1.

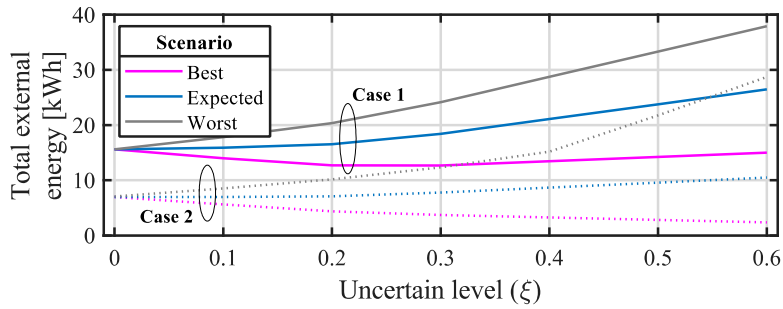

Figure 10. Total external energy in the studied cases for different scenarios of uncertainties.

5.3. Computational Burden

The proposed solution algorithm encompasses three stages, which sequentially solve three MILP optimization models. Stages 1 and 3 do not depend on the size of the P2P platform (i.e., the number of peers), as these stages solve individual HEM problems. On the other hand, the number of variables in Stage 2 increases with the number of peers partaking in the platform. In this sense, Stage 2 solves a conventional strategic offering/bidding problem with variables increasing in size with the number of peers. Therefore, the proposed solution techniques are not dramatically impacted by the number of peers, as only Stage 2 is sensitive to this parameter.

Preliminary experiments were run with up to 100 peers, showing that the computational time grows linearly with the number of prosumers in the platform. Even for a high number of prosumers, the total solution time keeps below 3 min in total, which is more than reasonable for day-ahead scheduling tools, thus showing that the proposed methodology scales well with the size of the system. Remarkably, it is worth noting that prosumer trading platforms normally involve few prosumers ($3 \div 10$) [54].

6. Conclusions and Future Works

A new HEM-based model for optimal participation of prosumers in competitive P2P platforms has been developed. The new proposal is casted as a three-stage methodology in which the first and last stages are focused on scheduling domestic assets, while the second stage decides the optimal offering/bidding strategy for the strategic prosumer. Moreover, the last stage incorporates uncertainties through interval notation and equivalent scenarios, resulting in a final result immune against uncertainties.

The new methodology was tested on a benchmark four-prosumer platform. The results evidenced that the proposed procedure maximizes the participation of the strategic prosumer in the platform. This feature enables monetary opportunities from P2P trading. The role of storage systems was also highlighted, showing that this kind of device allows users to export energy even when PV generation is null. It propitiates a higher participation of the prosumer in energy trading even at noon. The effect of uncertainties in the final result was also discussed, showing that the total energy acquired from external agents increases with the so-called uncertain level.

The new proposal may be valuable to maximize economic opportunities in competitive P2P platforms formed by prosumers, but also other agents like distributed generators. Due to the expected emergence of smart communications and local markets, the developed methodology might be implanted in different smart homes in order to encourage users to partake in local market arrangements. The foundations of the developed methodology are easily adaptable to other structures involving P2P trading, like microgrid clusters or energy communities. Future work should be focused on this research direction.

Author Contributions: Conceptualization, M.T.-V., H.M.H. and F.J.; data curation, A.A.Z. and F.J.; formal analysis, M.T.-V. and H.M.H.; funding acquisition, F.J.; investigation, A.A.Z. and M.T.-V.; methodology, M.T.-V.; project administration, F.J.; resources, H.M.H. and F.J.; software, A.A.Z.; supervision, H.M.H. and F.J.; validation, M.T.-V.; visualization, F.J.; writing—original draft, A.A.Z. and M.T.-V.; writing—review and editing, A.A.Z. and M.T.-V. All authors have read and agreed to the published version of the manuscript.

Funding: This research received no external funding.

Data Availability Statement: Data are made available upon request.

Conflicts of Interest: The authors declare no conflicts of interest.

Nomenclature

Indices (Set)	
i, j $(\mathbb{Q})$	Prosumer
t $(\mathbb{T})$	Time
a $(\mathbb{A}_i^I / \mathbb{A}_{i^*}^{NI})$	Interruptible/non − interruptible appliances of the i^{th} prosumer
Θ	Time window of a controllable appliance or electric vehicle
ω (Ω)	Scenario
Superscripts	
PV	Photovoltaic
BES	Battery energy storage
EV	Electric vehicle
$HVAC$	Heating–ventilation–air conditioner
c/d	Charging/discharging mode of storage systems
$heat/cool$	Heating/cooling mode of heating–ventilation–air conditioner units
$Air, in/out$	Indoor/outdoor air
sp	Set-point
$P2P$	Peer-to-peer transactions
Ext	External
$\underline{(\cdot)}/\overline{(\cdot)}$	Minimum/maximum value

Constants and parameters	
Δt	Time step [h]
η	Efficiency [pu]
$\varepsilon_{i,0}^{EV}$	Initial state − of − charge of the electric vehicle of the i^{th} prosumer [kWh]
θ	Temperature [°C]
m	Mass [kg]
Q	Heat capacity [kJ/(kg·°C)]
R	Thermal resistance of the building [J/°C]
COP	Coefficient of performance [-]
DC	Duty cycle [h]
α	Offer/bid price [$/kWh]
M	Large positive number (~10^5) [-]
Decision variables	
p	Power [kW]
y	Commitment status [Binary]
ε	Energy [kWh]
on/off	On/off status of a controllable appliance [Binary]
$p_{i\leftarrow}/p_{i\rightarrow}$	Power imported/exported by the i^{th} prosumer [kW]
$p_{i\rightarrow j}^{P2P}$	Power exported by the i^{th} prosumer to the j^{th} peer through peer-to-peer trade [kW]
λ_{i-j}^{P2P}	Clearing price for peer − to − peer trade between the ij^{th} pair of prosumers [$/kWh]
$\overline{\mu}_{i\rightarrow}$, $\overline{\mu}_{i\leftarrow}$	Dual variable for the maximum exportable/importable power of prosumer i [$/kWh]
$\underline{\mu}_{i\rightarrow j}$, $\underline{\mu}_{i\leftarrow j}$	Dual variable for the minimum exportable/importable power of prosumer i [$/kWh]
ψ	Auxiliary variable for linearization of complementarity constraints [Binary]

Appendix A. Derivation of the Stationary Constraints (25) and (26)

The Lagrangian function of (21) is given by the following:

$$\mathcal{L}\left(p_{i\rightarrow j,t}^{P2P}, p_{i\leftarrow j,t}^{P2P}\right) = \sum_{t\in\mathbb{T}}\sum_{i\in\mathbb{Q}}\sum_{\substack{j\in\mathbb{Q}\\ j\neq i}}\left\{\begin{array}{c} \alpha_{i,t}^{P2P}\cdot\left(p_{i\rightarrow j,t}^{P2P}-p_{i\leftarrow j,t}^{P2P}\right)+\lambda_{i-j,t}^{P2P}\cdot\left(p_{i\rightarrow j,t}^{P2P}-p_{j\leftarrow i,t}^{P2P}\right) \\ -\underline{\mu}_{i\rightarrow j,t}\cdot p_{i\rightarrow j,t}^{P2P}-\underline{\mu}_{i\leftarrow j,t}\cdot p_{i\leftarrow j,t}^{P2P} \\ +\overline{\mu}_{i\rightarrow,t}\cdot\left(p_{i\rightarrow j,t}^{P2P}-\overline{p}_{i\rightarrow,t}\right)+\overline{\mu}_{i\leftarrow,t}\cdot\left(p_{i\leftarrow j,t}^{P2P}-\overline{p}_{i\leftarrow,t}\right) \end{array}\right\} \quad \text{(A1)}$$

The stationary constraints of the MPCC problem described in Section 3 (25) and (26) are obtained by equaling the first partial derivatives of (A1) to zero, as follows:

$$\nabla\mathcal{L}|p_{i\rightarrow j,t}^{P2P}=0\rightarrow\alpha_{i,t}^{P2P}+\lambda_{i-j,t}^{P2P}-\underline{\mu}_{i\rightarrow j,t}+\overline{\mu}_{i\rightarrow,t}=0;\ \forall i,j\in\mathbb{Q}\backslash j\neq i\wedge t\in\mathbb{T} \quad \text{(A2)}$$

$$\nabla\mathcal{L}|p_{j\leftarrow i,t}^{P2P}=0\rightarrow-\alpha_{i,t}^{P2P}-\lambda_{i-j,t}^{P2P}-\underline{\mu}_{i\leftarrow j,t}+\overline{\mu}_{i\leftarrow,t}=0;\ \forall i,j\in\mathbb{Q}\backslash j\neq i\wedge t\in\mathbb{T} \quad \text{(A3)}$$

Appendix B. Linearization of (21)

Applying the strong duality theorem to (21) yields the following:

$$\sum_{t\in\mathbb{T}}\sum_{i\in\mathbb{Q}}\left\{\sum_{\substack{j\in\mathbb{Q}\\ j\neq i}}\left\{\alpha_{i,t}^{P2P}\cdot\left(p_{i\leftarrow j,t}^{P2P}-p_{i\rightarrow j,t}^{P2P}\right)\right\}\right\}=\sum_{t\in\mathbb{T}}\sum_{i\in\mathbb{Q}}\left\{-\overline{\mu}_{i\rightarrow,t}\cdot\overline{p}_{i\rightarrow,t}-\overline{\mu}_{i\leftarrow,t}\cdot\overline{p}_{i\leftarrow,t}\right\} \quad \text{(A4)}$$

The right-hand side of (A4) can be rewritten using (25) and (26), as follows:

$$\sum_{t\in\mathbb{T}}\sum_{i\in\mathbb{Q}}\sum_{\substack{j\in\mathbb{Q}\\ j\neq i}}\left\{\begin{array}{c}\alpha_{i,t}^{P2P}\cdot p_{i\to j,t}^{P2P}+\lambda_{i-j,t}^{P2P}\cdot p_{i\to j,t}^{P2P}\\ -\underline{\mu}_{i\to j,t}\cdot p_{i\to j,t}^{P2P}+\overline{\mu}_{i\to,t}\cdot p_{i\to j,t}^{P2P}\end{array}\right\}=0 \tag{A5}$$

$$\sum_{t\in\mathbb{T}}\sum_{i\in\mathbb{Q}}\sum_{\substack{j\in\mathbb{Q}\\ j\neq i}}\left\{\begin{array}{c}-\alpha_{i,t}^{P2P}\cdot p_{i\leftarrow j,t}^{P2P}-\lambda_{i-j,t}^{P2P}\cdot p_{i\leftarrow j,t}^{P2P}\\ -\underline{\mu}_{i\leftarrow j,t}\cdot p_{i\leftarrow j,t}^{P2P}+\overline{\mu}_{i\leftarrow,t}\cdot p_{i\leftarrow j,t}^{P2P}\end{array}\right\}=0 \tag{A6}$$

From complementarity conditions (27) and (28), the following equalities hold:

$$\begin{array}{l}0\le\overline{\mu}_{i\to,t}\perp\left(\overline{p}_{i\to,t}-\sum\limits_{\substack{j\in\mathbb{Q}\\ j\neq i}}p_{i\to j,t}^{P2P}\right)\ge 0\\ 0\le\overline{\mu}_{i\leftarrow,t}\perp\left(\overline{p}_{i\leftarrow,t}-\sum\limits_{\substack{j\in\mathbb{Q}\\ j\neq i}}p_{i\leftarrow j,t}^{P2P}\right)\ge 0\\ \forall i\in\mathbb{Q}\wedge t\in\mathbb{T}\end{array}\rightarrow\begin{array}{l}\overline{\mu}_{i\to,t}\cdot\overline{p}_{i\to,t}=\overline{\mu}_{i\to,t}\cdot\sum\limits_{\substack{j\in\mathbb{Q}\\ j\neq i}}p_{i\to j,t}^{P2P}\\ \overline{\mu}_{i\leftarrow,t}\cdot\overline{p}_{i\leftarrow,t}=\overline{\mu}_{i\leftarrow,t}\cdot\sum\limits_{\substack{j\in\mathbb{Q}\\ j\neq i}}p_{i\leftarrow j,t}^{P2P}\end{array}; \tag{A7}$$

$$\begin{array}{l}0\le\underline{\mu}_{i\to j,t}\perp p_{i\to j,t}^{P2P}\ge 0\\ 0\le\underline{\mu}_{i\leftarrow j,t}\perp p_{i\leftarrow j,t}^{P2P}\ge 0\end{array}\rightarrow\begin{array}{l}\underline{\mu}_{i\to j,t}\cdot p_{i\to j,t}^{P2P}=0\\ \underline{\mu}_{i\leftarrow j,t}\cdot p_{i\leftarrow j,t}^{P2P}=0\end{array};\ \forall i,j\in\mathbb{Q}\backslash j\neq i\wedge t\in\mathbb{T} \tag{A8}$$

Replacing (A7) and (A8) in (A5) and (A6), respectively, one obtains the following:

$$\sum_{t\in\mathbb{T}}\sum_{i\in\mathbb{Q}}\left\{\begin{array}{c}\sum\limits_{\substack{j\in\mathbb{Q}\\ j\neq i}}\left\{\begin{array}{c}\alpha_{i,t}^{P2P}\cdot p_{i\to j,t}^{P2P}\\ +\lambda_{i-j,t}^{P2P}\cdot p_{i\to j,t}^{P2P}\end{array}\right\}\\ +\overline{\mu}_{i\to,t}\cdot\overline{p}_{i\to,t}\end{array}\right\}=0 \tag{A9}$$

$$\sum_{t\in\mathbb{T}}\sum_{i\in\mathbb{Q}}\left\{\begin{array}{c}\sum\limits_{\substack{j\in\mathbb{Q}\\ j\neq i}}\left\{\begin{array}{c}-\alpha_{i,t}^{P2P}\cdot p_{i\leftarrow j,t}^{P2P}\\ -\lambda_{i-j,t}^{P2P}\cdot p_{i\leftarrow j,t}^{P2P}\end{array}\right\}\\ +\overline{\mu}_{i\leftarrow,t}\cdot\overline{p}_{i\leftarrow,t}\end{array}\right\}=0 \tag{A10}$$

Rearranging (A9) and (A10) one obtains the following:

$$\sum_{t\in\mathbb{T}}\sum_{i\in\mathbb{Q}}\sum_{\substack{j\in\mathbb{Q}\\ j\neq i}}\alpha_{i,t}^{P2P}\cdot p_{i\to j,t}^{P2P}=-\sum_{t\in\mathbb{T}}\sum_{i\in\mathbb{Q}}\left\{\begin{array}{c}\sum\limits_{\substack{j\in\mathbb{Q}\\ j\neq i}}\left\{\lambda_{i-j,t}^{P2P}\cdot p_{i\to j,t}^{P2P}\right\}\\ +\overline{\mu}_{i\to,t}\cdot\overline{p}_{i\to,t}\end{array}\right\} \tag{A11}$$

$$-\sum_{t\in\mathbb{T}}\sum_{i\in\mathbb{Q}}\sum_{\substack{j\in\mathbb{Q}\\ j\neq i}}\alpha_{i,t}^{P2P}\cdot p_{i\leftarrow j,t}^{P2P}=\sum_{t\in\mathbb{T}}\sum_{i\in\mathbb{Q}}\left\{\begin{array}{c}\sum\limits_{\substack{j\in\mathbb{Q}\\ j\neq i}}\left\{+\lambda_{i-j,t}^{P2P}\cdot p_{i\leftarrow j,t}^{P2P}\right\}\\ -\overline{\mu}_{i\leftarrow,t}\cdot\overline{p}_{i\leftarrow,t}\end{array}\right\} \tag{A12}$$

After particularizing (A11) and (A12) for $i=i^*$ one obtains the following:

$$\sum_{t\in\mathbb{T}}\sum_{\substack{j\in\mathbb{Q}\\ j\neq i^*}}\alpha_{i^*,t}^{P2P}\cdot p_{i^*\to j,t}^{P2P}=-\sum_{t\in\mathbb{T}}\left\{\sum_{\substack{j\in\mathbb{Q}\\ j\neq i^*}}\left\{\lambda_{i^*-j,t}^{P2P}\cdot p_{i^*\to j,t}^{P2P}\right\}+\overline{\mu}_{i^*\to,t}\cdot\overline{p}_{i^*\to,t}\right\} \tag{A13}$$

$$-\sum_{t\in\mathbb{T}}\sum_{\substack{j\in\mathbb{Q}\\ j\neq i^*}}\alpha^{P2P}_{i^*,t}\cdot p^{P2P}_{i^*\leftarrow j,t}=\sum_{t\in\mathbb{T}}\left\{\sum_{\substack{j\in\mathbb{Q}\\ j\neq i^*}}\left\{\lambda^{P2P}_{i^*-j,t}\cdot p^{P2P}_{i^*\leftarrow j,t}\right\}+\overline{\mu}_{i^*\leftarrow,t}\cdot\overline{p}_{i^*\leftarrow,t}\right\} \tag{A14}$$

Replacing (A13) and (A14) in (A4) yields the following:

$$\sum_{t\in\mathbb{T}}\left\{\begin{array}{l}\sum\limits_{\substack{j\in\mathbb{Q}\\ j\neq i^*}}\lambda^{P2P}_{i^*-j,t}\cdot\left(p^{P2P}_{i^*\leftarrow j,t}-p^{P2P}_{i^*\rightarrow j,t}\right)\\ -\overline{\mu}_{i^*\leftarrow,t}\cdot\overline{p}_{i^*\leftarrow,t}-\overline{\mu}_{i^*\rightarrow,t}\cdot\overline{p}_{i^*\rightarrow,t}\\ +\sum\limits_{\substack{i\in\mathbb{Q}\\ i\neq i^*}}\sum\limits_{\substack{j\in\mathbb{Q}\\ j\neq i^*}}\alpha^{P2P}_{i,t}\cdot\left(p^{P2P}_{i\leftarrow j,t}-p^{P2P}_{i\rightarrow j,t}\right)\end{array}\right\}=-\sum_{t\in\mathbb{T}}\sum_{i\in\mathbb{Q}}\left\{\begin{array}{l}\overline{\mu}_{i\rightarrow,t}\cdot\overline{p}_{i\rightarrow,t}+\\ \overline{\mu}_{i\leftarrow,t}\cdot\overline{p}_{i\leftarrow,t}\end{array}\right\} \tag{A15}$$

And finally rearranging (A15), one obtains the following:

$$\sum_{t\in\mathbb{T}}\sum_{\substack{j\in\mathbb{Q}\\ j\neq i^*}}\lambda^{P2P}_{i^*-j,t}\cdot\left(p^{P2P}_{i^*\rightarrow j,t}-p^{P2P}_{i^*\leftarrow j,t}\right)=\sum_{t\in\mathbb{T}}\left\{\begin{array}{l}\sum\limits_{\substack{i\in\mathbb{Q}\\ i\neq i^*}}\sum\limits_{\substack{j\in\mathbb{Q}\\ j\neq i^*}}\alpha^{P2P}_{i,t}\cdot\left(p^{P2P}_{i\leftarrow j,t}-p^{P2P}_{i\rightarrow j,t}\right)+\\ \sum\limits_{\substack{i\in\mathbb{Q}\\ i\neq i^*}}\left\{\overline{\mu}_{i\rightarrow,t}\cdot\overline{p}_{i\rightarrow,t}+\overline{\mu}_{i\leftarrow,t}\cdot\overline{p}_{i\leftarrow,t}\right\}\end{array}\right\} \tag{A16}$$

References

1. Guerrero, J.; Gebbran, D.; Mhanna, S.; Chapman, A.C.; Verbič, G. Towards a transactive energy system for integration of distributed energy resources: Home energy management, distributed optimal power flow, and peer-to-peer energy trading. *Renew. Sustain. Energy Rev.* **2020**, *132*, 110000. [CrossRef]
2. Soriano, L.A.; Avila, M.; Ponce, P.; de Jesús Rubio, J.; Molina, A. Peer-to-peer energy trades based on multi-objective optimization. *Int. J. Electr. Power Energy Syst.* **2021**, *131*, 107017. [CrossRef]
3. Lilla, S.; Orozco, C.; Borghetti, A.; Napolitano, F.; Tossani, F. Day-Ahead Scheduling of a Local Energy Community: An Alternating Direction Method of Multipliers Approach. *IEEE Trans. Power Syst.* **2020**, *35*, 1132–1142. [CrossRef]
4. Tostado-Véliz, M.; Kamel, S.; Hasanien, H.M.; Turky, R.A.; Jurado, F. Optimal energy management of cooperative energy communities considering flexible demand, storage and vehicle-to-grid under uncertainties. *Sustain. Cities Soc.* **2022**, *84*, 104019. [CrossRef]
5. Jo, H.-C.; Byeon, G.; Kim, J.-Y.; Kim, S.-K. Optimal Scheduling for a Zero Net Energy Community Microgrid With Customer-Owned Energy Storage Systems. *IEEE Trans. Power Syst.* **2021**, *36*, 2273–2280. [CrossRef]
6. Gomes, I.; Bot, K.; Ruano, M.G.; Ruano, A. Recent Techniques Used in Home Energy Management Systems: A Review. *Energies* **2022**, *15*, 2866. [CrossRef]
7. Kim, H.; Lee, S.K.; Kim, H.; Kim, H. Implementing home energy management system with UPnP and mobile applications. *Comput. Commun.* **2012**, *36*, 51–62. [CrossRef]
8. Chavali, P.; Yang, P.; Nehorai, A. A Distributed Algorithm of Appliance Scheduling for Home Energy Management System. *IEEE Trans. Smart Grid* **2014**, *5*, 282–290. [CrossRef]
9. Rastegar, M.; Fotuhi-Firuzabad, M.; Zareipour, H. Home energy management incorporating operational priority of appliances. *Int. J. Electr. Power Energy Syst.* **2016**, *74*, 286–292. [CrossRef]
10. Anvari-Moghaddam, A.; Monsef, H.; Rahimi-Kian, A. Optimal Smart Home Energy Management Considering Energy Saving and a Comfortable Lifestyle. *IEEE Trans. Smart Grid* **2015**, *6*, 324–332. [CrossRef]
11. Paterakis, N.G.; Erdinç, O.; Bakirtzis, A.G.; Catalão, J.P.S. Optimal Household Appliances Scheduling Under Day-Ahead Pricing and Load-Shaping Demand Response Strategies. *IEEE Trans. Ind. Inform.* **2015**, *11*, 1509–1519. [CrossRef]
12. Shafie-Khah, M.; Siano, P. A Stochastic Home Energy Management System Considering Satisfaction Cost and Response Fatigue. *IEEE Trans. Ind. Inform.* **2018**, *14*, 629–638. [CrossRef]
13. Tostado-Véliz, M.; Kamel, S.; Aymen, F.; Jurado, F. A novel hybrid lexicographic-IGDT methodology for robust multi-objective solution of home energy management systems. *Energy* **2022**, *253*, 124146. [CrossRef]
14. Javadi, M.S.; Gough, M.; Lotfi, M.; Nezhad, A.E.; Santos, S.F.; Catalão, J.P.S. Optimal self-scheduling of home energy management system in the presence of photovoltaic power generation and batteries. *Energy* **2020**, *210*, 118568. [CrossRef]
15. Javadi, M.S.; Nezhad, A.E.; Nardelli, P.H.; Gough, M.; Lotfi, M.; Santos, S.; Catalão, J.P. Self-scheduling model for home energy management systems considering the end-users discomfort index within price-based demand response programs. *Sustain. Cities Soc.* **2021**, *68*, 102792. [CrossRef]

16. Wang, X.; Li, F.; Dong, J.; Olama, M.M.; Zhang, Q.; Shi, Q.; Kuruganti, T. Tri-Level Scheduling Model Considering Residential Demand Flexibility of Aggregated HVACs and EVs Under Distribution LMP. *IEEE Trans. Smart Grid* **2021**, *12*, 3990–4002. [CrossRef]
17. Rücker, F.; Schoeneberger, I.; Wilmschen, T.; Sperling, D.; Haberschusz, D.; Figgener, J.; Sauer, D.U. Self-sufficiency and charger constraints of prosumer households with vehicle-to-home strategies. *Appl. Energy* **2022**, *317*, 119060. [CrossRef]
18. Ali, A.; Aftab, A.; Akram, M.N.; Awan, S.; Muqeet, H.A.; Arfeen, Z.A. Residential Prosumer Energy Management System with Renewable Integration Considering Multi-Energy Storage and Demand Response. *Sustainability* **2024**, *16*, 2156. [CrossRef]
19. Aljohani, T.M. Multilayer Iterative Stochastic Dynamic Programming for Optimal Energy Management of Residential Loads with Electric Vehicles. *Int. J. Energy Res.* **2024**, *2024*, 6842580. [CrossRef]
20. Tostado-Véliz, M.; Gurung, S.; Jurado, F. Efficient solution of many-objective Home Energy Management systems. *Int. J. Electr. Power Energy Syst.* **2022**, *136*, 107666. [CrossRef]
21. Deng, Y.; Zhang, Y.; Luo, F.; Ranzi, G. Many-Objective HEMS Based on Multi-Scale Occupant Satisfaction Modelling and Second-Life BESS Utilization. *IEEE Trans. Sustain. Energy* **2022**, *13*, 934–947. [CrossRef]
22. Dinh, H.T.; Lee, K.-H.; Kim, D. Supervised-learning-based hour-ahead demand response for a behavior-based home energy management system approximating MILP optimization. *Appl. Energy* **2022**, *321*, 119382. [CrossRef]
23. Yang, J.; Huang, G.; Wei, C. Privacy-aware electricity scheduling for home energy management system. *Peer-to-Peer Netw. Appl.* **2018**, *11*, 309–317. [CrossRef]
24. Long, C.; Wu, J.; Zhou, Y.; Jenkins, N. Peer-to-peer energy sharing through a two-stage aggregated battery control in a community Microgrid. *Appl. Energy* **2018**, *226*, 261–276. [CrossRef]
25. Paudel, A.; Chaudhari, K.; Long, C.; Gooi, H.B. Peer-to-Peer Energy Trading in a Prosumer-Based Community Microgrid: A Game-Theoretic Model. *IEEE Trans. Ind. Electron.* **2019**, *66*, 6087–6097. [CrossRef]
26. Feng, C.; Wen, F.; You, S.; Li, Z.; Shahnia, F.; Shahidehpour, M. Coalitional Game-Based Transactive Energy Management in Local Energy Communities. *IEEE Trans. Power Syst.* **2020**, *35*, 1729–1740. [CrossRef]
27. Daneshvar, M.; Mohammadi-Ivatloo, B.; Zare, K.; Asadi, S.; Anvari-Moghaddam, A. A Novel Operational Model for Interconnected Microgrids Participation in Transactive Energy Market: A Hybrid IGDT/Stochastic Approach. *IEEE Trans. Ind. Inform.* **2021**, *17*, 4025–4035. [CrossRef]
28. Mehrjerdi, H. Peer-to-peer home energy management incorporating hydrogen storage system and solar generating units. *Renew. Energy* **2020**, *156*, 183–192. [CrossRef]
29. Park, D.-H.; Park, J.-B.; Lee, K.Y.; Son, S.-Y.; Roh, J.H. A Bidding-Based Peer-to-Peer Energy Transaction Model Considering the Green Energy Preference in Virtual Energy Community. *IEEE Access* **2021**, *9*, 87410–87419. [CrossRef]
30. Khorasany, M.; Razzaghi, R.; Gazafroudi, A.S. Two-stage mechanism design for energy trading of strategic agents in energy communities. *Appl. Energy* **2021**, *295*, 117036. [CrossRef]
31. Javadi, M.S.; Gough, M.; Nezhad, A.E.; Santos, S.F.; Shafie-Khah, M.; Catalão, J.P.S. Pool trading model within a local energy community considering flexible loads, photovoltaic generation and energy storage systems. *Sustain. Cities Soc.* **2022**, *79*, 103747. [CrossRef]
32. Mu, C.; Ding, T.; Sun, Y.; Huang, Y.; Li, F.; Siano, P. Energy Block-Based Peer-to-Peer Contract Trading With Secure Multi-Party Computation in Nanogrid. *IEEE Trans. Smart Grid* **2022**, *13*, 4759–4772. [CrossRef]
33. Gough, M.; Santos, S.F.; Almeida, A.; Lotfi, M.; Javadi, M.S.; Fitiwi, D.Z.; Catalão, J.P. Blockchain-Based Transactive Energy Framework for Connected Virtual Power Plants. *IEEE Trans. Ind. Appl.* **2022**, *58*, 986–995. [CrossRef]
34. Nezamabadi, H.; Vahidinasab, V. Arbitrage Strategy of Renewable-Based Microgrids via Peer-to-Peer Energy-Trading. *IEEE Trans. Sustain. Energy* **2021**, *12*, 1372–1382. [CrossRef]
35. Stanescu, D.; Enache, F.; Popescu, F. Smart Non-Intrusive Appliance Load-Monitoring System Based on Phase Diagram Analysis. *Smart Cities* **2024**, *7*, 1936–1949. [CrossRef]
36. Mandal, S.; Das, B.K.; Hoque, N. Optimum sizing of a stand-alone hybrid energy system for rural electrification in Bangladesh. *J. Clean. Prod.* **2018**, *200*, 12–27. [CrossRef]
37. Tostado-Véliz, M.; Mouassa, S.; Jurado, F. A MILP framework for electricity tariff-choosing decision process in smart homes considering 'Happy Hours' tariffs. *Int. J. Electr. Power Energy Syst.* **2021**, *131*, 107139. [CrossRef]
38. Tostado-Véliz, M.; Jordehi, A.R.; Mansouri, S.A.; Jurado, F. Day-ahead scheduling of 100% isolated communities under uncertainties through a novel stochastic-robust model. *Appl. Energy* **2022**, *328*, 120257. [CrossRef]
39. Negarestani, S.; Fotuhi-Firuzabad, M.; Rastegar, M.; Rajabi-Ghahnavieh, A. Optimal Sizing of Storage System in a Fast Charging Station for Plug-in Hybrid Electric Vehicles. *IEEE Trans. Transp. Electrif.* **2016**, *2*, 443–453. [CrossRef]
40. Maher, K.; Bouaiza, A.; Amin, R. Understanding the heat generation mechanisms and the interplay between joule heat and entropy effects as a function of state of charge in lithium-ion batteries. *J. Power Sources* **2024**, *623*, 235504. [CrossRef]
41. Liang, Z.; Chung, C.Y.; Zhang, W.; Wang, Q.; Lin, W.; Wang, C. Enabling High-Efficiency Economic Dispatch of Hybrid AC/DC Networked Microgrids: Steady-State Convex Bi-Directional Converter Models. *IEEE Trans. Smart Grid* 2024, *early access*. [CrossRef]
42. Boumaiza, A. A blockchain-centric P2P trading framework incorporating carbon and energy trades. *Energy Strategy Rev.* **2024**, *54*, 101466. [CrossRef]
43. Wang, X.; Li, F.; Zhang, Q.; Shi, Q.; Wang, J. Profit-Oriented BESS Siting and Sizing in Deregulated Distribution Systems. *IEEE Trans. Smart Grid.* **2022**, *14*, 1528–1540. [CrossRef]

44. Nekouei, E.; Alpcan, T.; Chattopadhyay, D. Game-Theoretic Frameworks for Demand Response in Electricity Markets. *IEEE Trans. Smart Grid* **2015**, *6*, 748–758. [CrossRef]
45. Jabr, R.A.; Džafić, I.; Pal, B.C. Robust Optimization of Storage Investment on Transmission Networks. *IEEE Trans. Power Syst.* **2015**, *30*, 531–539. [CrossRef]
46. Fu, Y.; Zhang, Z.; Li, Z.; Mi, Y. Energy Management for Hybrid AC/DC Distribution System With Microgrid Clusters Using Non-Cooperative Game Theory and Robust Optimization. *IEEE Trans. Smart Grid* **2020**, *11*, 1510–1525. [CrossRef]
47. Kleinert, T.; Labbe, M.; Plein, F.; Schmidt, M. There's no free lunch: On the hardness of choosing a correct big-M in bilevel optimization. *Oper. Res.* **2020**, *68*, 1716–1721. [CrossRef]
48. Baringo, L.; Conejo, A.J. Strategic Offering for a Wind Power Producer. *IEEE Trans. Power Syst.* **2013**, *28*, 4645–4654. [CrossRef]
49. Zhuo, Z.; Du, E.; Zhang, N.; Kang, C.; Xia, Q.; Wang, Z. Incorporating Massive Scenarios in Transmission Expansion Planning With High Renewable Energy Penetration. *IEEE Trans. Power Syst.* **2020**, *35*, 1061–1074. [CrossRef]
50. Tostado-Véliz, M.; Kamel, S.; Hasanien, H.M.; Arévalo, P.; Turky, R.A.; Jurado, F. A stochastic-interval model for optimal scheduling of PV-assisted multi-mode charging stations. *Energy* **2022**, *253*, 124219. [CrossRef]
51. Wang, X.; Li, F.; Zhao, J.; Olama, M.; Dong, J.; Shuai, H.; Kuruganti, T. Tri-level hybrid interval-stochastic optimal scheduling for flexible residential loads under GAN-assisted multiple uncertainties. *Int. J. Electr. Power Energy Syst.* **2023**, *146*, 108672. [CrossRef]
52. Nezamabadi, H.; Vahidinasab, V. Market bidding strategy of the microgrids considering demand response and energy storage potential flexibilities. *IET Gener. Transm. Distrib.* **2019**, *13*, 1346–1357. [CrossRef]
53. Gurobi Optimizer Reference Manual. Available online: https://www.gurobi.com/wp-content/plugins/hd_documentations/documentation/9.1/refman.pdf (accessed on 30 October 2024).
54. Vespermann, N.; Hamacher, T.; Kazempour, J. Risk Trading in Energy Communities. *IEEE Trans. Smart Grid* **2021**, *12*, 1249–1263. [CrossRef]